Available online at www.sciencedirect.com

ScienceDirect

Procedia CIRP 102 (2021) 138–143

www.elsevier.com/locate/procedia

18th CIRP Conference on Modeling of Machining Operations

A new approach for local cutting force modeling enabling the transfer between different milling conditions and tool geometries

Andreas Hilligardt*, Felicitas Böhland, Jan Klose, Michael Gerstenmeyer, Volker Schulze

wbk Institute of Production Science, Kalrsuhe Institute of Technolgy (KIT), Kaiserstr. 12, 76131 Karlsruhe, Germany

* Corresponding author. Tel.: +49-721-608-42455; fax: +49-721-608-45004; *E-mail address:* andreas.hilligardt@kit.edu

Abstract

The modeling of modern high performance machining with intermittent cut and varying effective cutting parameters requires a flexible local cutting force prediction. Due to complex tool geometries and varying cutting conditions without a rigid reference system new approaches for the local cutting force decomposition are applied, investigated and compared. The force decompositions are based on the separation of the effective cutting speed into normal and tangential components to adequately consider the locally acting mechanisms. Regression models based on the effective cutting parameters are defined to compare and validate the local force decomposition. A high feed peripheral milling experiment with specific cutting force measurement is presented to develop the regression models. An extensive cutting force database for AISI 5115 is created by tool geometry and process control variable variations. The effective cutting conditions are calculated through geometric penetration simulation. Considering the tool deflection in the simulation achieves a high regression accuracy even with low chip thicknesses. This is especially important for the cutting force prediction of finishing processes. The resulting regression cutting force models and force decompositions are rated based on the applicability to different tool geometries, like a ball end mill.

Keywords: geometric modelling; cutting, force, kinematic, simulation;

1. Introduction

Cutting force modeling is essential to improve accuracy and productivity in machining processes. With adequate force prediction fundamental data for tool deflection, tool wear, quality of the workpiece and appropriate choice of process parameters can be generated. Due to complexity of processes and tool geometries there is an increased requirement for flexible and simple force prediction models. The simulation of cutting forces has been implemented by many researchers using three main approaches: analytical, numerical and mechanistic modelling [1]. The analytical models can not only predict cutting forces, but also stresses, strains and strain rate. But due to the necessity to determine very detailed process conditions the accuracy of the approach is limited. Analytical models are usually based on an early work by Merchant [2]. The numerical approaches simulate the machining process based on mechanisms of continuum mechanics. For the determination of parameters flow of material, deformation rates and friction coefficients are needed which are difficult to determine [3]. Mainly the models use Johnson Cook equations for different materials and the Coulomb's model for friction coefficients [4]. The mechanistic modeling relates cutting force components to geometric parameters by fitting coefficients. It can be applied to different tool geometries and workpieces but specific tuning is necessary requiring a multitude of experiments [5]. Mainly two models are used. One where shearing and friction are described with only one coefficient. The advantage is a fast implementation and generally sufficient results [6]. This model has been implemented to ball end mills by researchers like

10.1016/j.procir.2021.09.024

Altintas and Spence [7] and Lazoglu [8]. More complex models called dual mechanics approaches have separate coefficients for shearing and friction. An oblique cutting force model applied to ball nose end milling which was adopted successfully by many researchers was developed by Lee and Altintas [9]. The cutting force coefficients are determined by oblique or orthogonal cutting. Another approach is equating average cutting force with measured data to predict forces for a general end mill [10]. Engin and Altintas [5] presented a general mathematical model usable for different helical mills. Current models are often restricted to force prediction for similar tool geometries and process operations while requiring a huge data set. There are only few approaches enabling transferability. Denkena and Vehmeyer [11] used a polynomial regression for force modelling which is easily applicable and principally not restricted by tool shape or kinematics. But no validation with differing tool geometries is presented and the results show restrictions regarding different feed rates. To calculate local geometric parameters, needed for mechanistic models, dexel based simulations [12] or cutting tool trajectory based models [13] are common approaches.

The influence of tool deflection on real chip thickness and cutting forces is object of current research in micro milling. The real chip thickness is used to increase the cutting force prediction accuracy [14].

In this work an extended Kienzle [15] model is presented to enable a flexible and simply transferable cutting force prediction which can be used to forecast the forces in complex cutting processes with varying local process parameter for AISI 5115. To achieve this, the cutting force components are decomposed along the directions of local effective normal and sliding speeds. Evaluation of the machined surface enables the analysis and modeling of the real chip thickness, which varies due to deflection between the tool and the machined workpiece. For this, a high feed experiment preserving the machined surface is presented. The cutting force model is validated by transferring it from the high feed to classic up-milling experiments and from helix tools to a ball end mill.

Nomenclature

a_e	radial infeed
c_{tool}	tool stiffness
c_{setup}	combined stiffness of machines components, tool holder and workpiece clamping
F_x, F_y, F_z	force components in x, y and z direction
f_z	feed per tooth
h	chip thickness
K_i	specific force coefficients
$m_{i,j}$	force model exponentials
v_e	effective cutting speed
v_{ne}	effective normal speed
v_{rot}	rotational speed
v_{se}	effective sliding speed
α_{ne}	effective clearance angle
γ_{ne}	effective rake angle
λ	helix angle
Δy_{repeat}	machine repetitive positioning accuracy

2. High Feed Experiments

The experiments are performed by high feed cutting (HFC). The entire topography of one cut and its position relative to the precut can be analyzed by the selected feed, see Fig 1. Compared to conventional milling, the different kinematics enable a wide variation of local process parameters and the characteristics of up and down milling occur in a single cut.

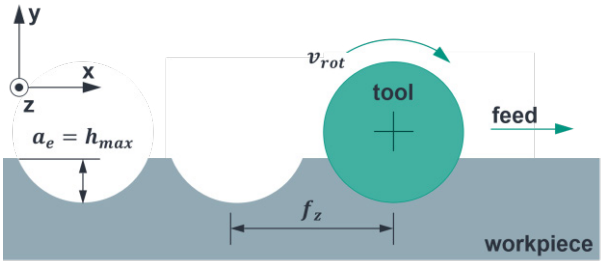

Fig. 1. Schematic illustration of the high feed process.

To reduce the frequency of tool interactions and compensate tool runout between pre and measurement cut, tools with one cutting edge are used. Another limit due to the frequency is the cutting speed. Thus the maximum rotational speed is set to 100 m/min. The cutting edge preparation, tools carbide, TiAlN-coating and the tool diameter of 12 mm are the same for the two tool geometries being used. One is a ball nose tool with a helix angle of 30° that changes towards the tool tip and the other a normal end mill with helix angle of 45°. The machined material is AISI 5115 and the sample dimensions are 150 mm length, 60 mm width and 10 mm processing height. All of the dry high feed peripheral milling tests were performed on a Heller MC16 machining center. Force measurement during the process is done by a three component dynamometer (Kistler Type 9255C). The signals are sampled with 10 kHz and a low-pass filter with 3 kHz is applied to reduce signal noise. The individual dynamic behavior of the experimental setup is analyzed by impulse hammer testing. Afterwards the three-dimensional inverse frequency response function is calculated and the diagonal of the matrix is applied to compensate the dynamic influences of the setup on the measured force signal. The measured forces are analyzed in the workpiece coordinate system, which is the dynamometers coordinate system, see Fig. 1. Due to uncertainties of the run in and run out of the individual sample, only 80 % of the measured signal is analyzed. Throughout this 80 % signal range the cutting force signal of an average cut is evaluated as time synchronous average for every sample and thus local measurement errors are eliminated. All experiments are performed with a precut by up milling. The cutting parameters for the precut are a rotational tool speed v_{rot} of 100 m/min, a feed per tooth f_z of 0.125 mm and a radial infeed a_e of 0.2 mm. The low infeed is selected to have a small tool deflection during the precut. Furthermore all workpiece samples are pretreated by another cut before the precut to compensate manufacturing and clamping defects. Thus, defined cutting condition for every precut can be guaranteed. The full design of experiments is presented in Fig. 2. The experimental points are varied over the rotational speed v_{rot} and the infeed a_e which is equivalent to the maximum

cutting thickness in this setup. The feed is adjusted to generate the same precut proportions for different infeed.

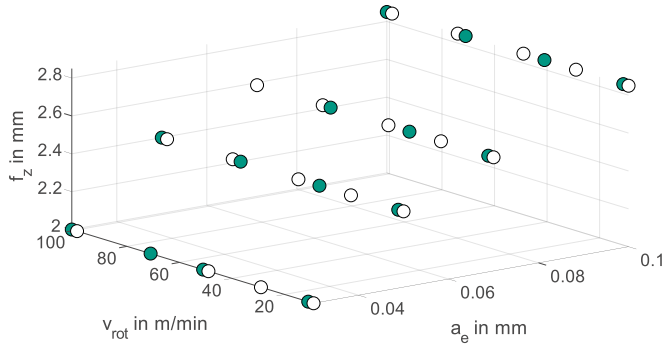

Fig. 2. Experimental design (filled point: λ = 30°, blank point: λ = 45°)

3. Modelling of cutting parameters

3.1. Geometric penetration simulation

In order to develop a fast and transferable cutting force model, an approach based on local geometric cutting parameters is chosen. To calculate the uncut chip thickness, a dexel based simulation similar to existing solutions is developed [12]. To improve computing accuracy and speed for the application of this geometric penetration simulation, some changes are implemented.

The cutting edge is discretized and normal vectors $\vec{K}$, normal rake face vectors $\vec{R}$, normal clearance face vectors $\vec{C}$ and the local tangential vectors $\vec{T}$ of the cutting edge are defined for every discrete point. In the simulation the workpiece is modeled by a number of dexel, which end points are triangulated. In a first step the chip thickness is calculated along the cutting edge normal $\vec{K}$ on the rake face for every time step. This is shown in Fig. 3a in a two-dimensional view. Afterwards the workpiece dexel are trimmed against the triangulated sweep surface of the cutting edge in its current position and a time step bevor. In Fig. 3b this is shown in a top view.

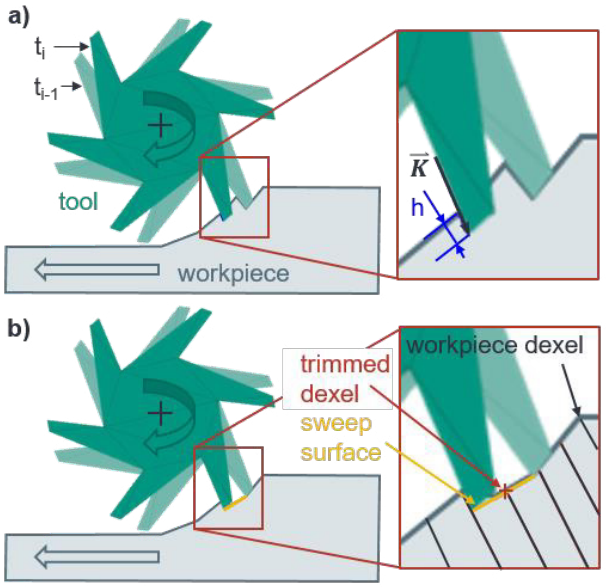

Fig. 3. 2D illustration of the penetration simulation: a) chip thickness calculation, b) workpiece trimming

To analyze the force components according to the process kinematics, the local speed vectors are determined. The relative speed between workpiece and cutting tool, which is equal to the resulting effective cutting speed $\overrightarrow{v_e}$, is divided into sliding speed tangential to the cutting edge $\overrightarrow{v_{se}}$ and the effective normal speed $\overrightarrow{v_{ne}}$, see Fig. 4.

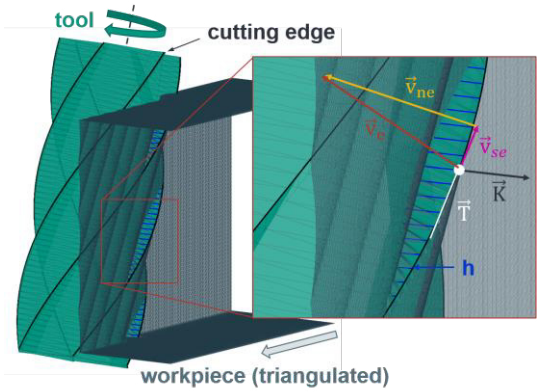

Fig. 4. Speed decomposition on the cutting edge

$$\overrightarrow{v_{se}} = (\vec{T} \cdot \overrightarrow{v_e})\vec{T} \quad (1)$$

$$\overrightarrow{v_{ne}} = \overrightarrow{v_e} - \overrightarrow{v_{se}} \quad (2)$$

The relative orientation of the effective normal speed $\overrightarrow{v_{ne}}$ and the local contour normal $\vec{K}$ as well as the normal of the clearance face $\vec{C}$ in the cutting edge normal plane give the effective normal rake γ_{ne} and clearance angle α_{ne}. This is of special interest for investigating processes with complex kinematics, like skiving, where angles are varying heavily [13].

$$\gamma_{ne} = -\arccos\left(\frac{\vec{K}\cdot\overrightarrow{v_{ne}}}{|\vec{K}|\cdot|\overrightarrow{v_{ne}}|}\right) + \frac{\pi}{2} \quad (3)$$

$$\alpha_{ne} = \arccos\left(\frac{\vec{C}\cdot\overrightarrow{v_{ne}}}{|\vec{C}|\cdot|\overrightarrow{v_{ne}}|}\right) - \frac{\pi}{2} \quad (4)$$

3.2. Modelling of deflection

One of the main advantages of the performed high feed experiments is preserving all of the machined surface in the measurement cut and parts of the precut. The machined topography is evaluated through a confocal microscope Nanofocus µsurf. An exemplary evaluation is shown in Fig. 5.

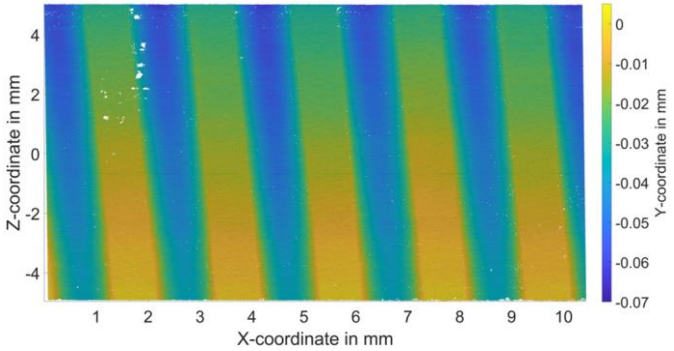

Fig. 5. Topography created in high feed process

To eliminate local measurement errors the topography average of three individual cuts is calculated, see Fig. 6. Due to the maximum distance between the precut surface and the measurement cut being equal to the maximum chip thickness, the real chip thickness can be determined easily. Along the width of the tool contact (z-axis) a change in cutting thickness is apparent. This is the result of different cutting forces in the precut and measurement cut, which lead to different deflections between workpiece and tool. The measurement cuts are performed with the same single tooth tools as the precut, therefore tool runout effects are the same in precut and measurement cut. Hence the real chip thickness is not influenced by the tool runout.

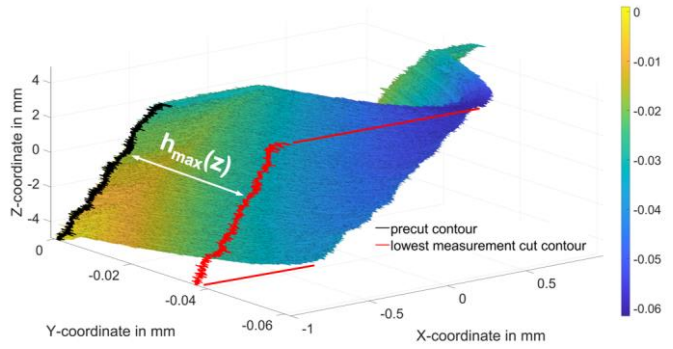

Fig. 6. Maximum cutting thickness in the 3D average surface

Deviations between the theoretical, simulated chip thickness and real chip thickness can be traced back to the repetitive positioning accuracy of the machine as well as force dependent deflections of machine components and the tool. To model the effective local cutting parameters, a simple deflection approach is implemented. The tool is divided in two segments – solid shaft and cutting zone – with different second moments of area. Tool deflection is then considered with a Euler-Bernoulli-Bending-Beam stiffness $c_{tool}(z)$ modeling of the tool. The deflection of the machine components, tool holder and workpiece clamping is considered with a three dimensional linear stiffness $c_{setup,x,y,z}$. For the evaluation of the real maximum chip thickness of all experimental points the second moment area of the cutting zones, the compliance and the individual machine repetitive positioning accuracy Δy_{repeat} can be determined through a least square optimization. Thus the model parameters are fitted so that the simulated resulting surface and cutting thickness match the measured topography of the experimental design. The carbide tools Young's modulus was assumed to be 585 GPa. This stiffness model results in a tool center point deflection depending on the measured cutting forces $F_{x,y,z}(z)$ and processing height z, as shown in formula 5.

$$\begin{bmatrix}\Delta x(z)\\ \Delta y(z)\\ \Delta z(z)\end{bmatrix} = \begin{bmatrix}\frac{F_x(z)}{c_{tool}(z)} + \frac{F_x(z)}{c_{setup,x}}\\ \frac{F_y(z)}{c_{tool}(z)} + \frac{F_y(z)}{c_{setup,y}} + \Delta y_{repeat}\\ \frac{F_z(z)}{c_{setup,z}}\end{bmatrix} \quad (5)$$

The deflection model is then used in the geometric penetration calculation to calculate the real chip thickness. By using the measured cutting force for every time step the individual deflection of the tool relative to the workpiece is calculated and applied before calculating the cutting parameters. The difference in maximum cutting thickness between an ideal rigid system and the deflected experimental setup is shown exemplary in Fig. 7. Due to different tool deflection in consecutive tool passes, the cutting thickness changes as the contact between tool and workpiece proceeds along the workpiece height (Z-coordinate).

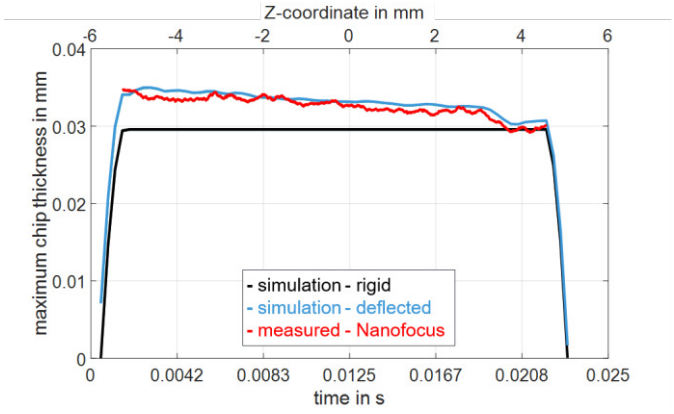

Fig. 7. Maximum simulated chip thickness along a typical HFC cut

4. Modelling of cutting force

The aim of this work is an accurate cutting force model with few individual regression parameters transferable to other applications. For this, different local force decompositions are implemented. Their effects on model accuracy and transferability to other tool geometries and process kinematics are evaluated and compared. Every model consists of three different local force components.

The first decomposition (DeCo-1) is using a simple cylindrical coordinate system for the tool. Hereby the first component is aligned tangentially to the tool diameter. The second component is radial to the cutting edge point and the third is directed along the tool axis without inclination around the helix angle. The second decomposition (DeCo-2) is similar to the work of Engin and Altintas [5]. Here the first component is normal to the rake face, the second tangential to the cutting edge and the third is perpendicular to the other two force components. The third decomposition (DeCo-3) is based on the resulting speed decompositions presented in chapter 3. Thereby the first two differential cutting force components are directed in the opposite direction of the effective normal speed and sliding speed. The third component is again perpendicular to the other two force components.

Based on the widespread cutting force modelling of Kienzle [15] a potential approach for the force components is implemented. In addition to the uncut chip thickness, the effective normal speed and sliding speed are considered.

$$\begin{bmatrix}dF_t\\ dF_r\\ dF_a\end{bmatrix} = \begin{bmatrix}K_t \cdot v_{ne}^{m_{tne}} \cdot v_{se}^{m_{tse}} \cdot h^{(1-m_t)}\\ K_r \cdot v_{ne}^{m_{rne}} \cdot v_{se}^{m_{rse}} \cdot h^{(1-m_r)}\\ K_a \cdot v_{ne}^{m_{ane}} \cdot v_{se}^{m_{ase}} \cdot h^{(1-m_a)}\end{bmatrix} \quad (6)$$

The deviation between modeled cutting forces and force measurements are calculated as least squares. With the MATLAB© integrated solver lsqnonlin the cutting force models are fitted to the experimental cutting force data based on the Levenberg-Marquardt Algorithm [16].

5. Results and Validation

The modelling accuracies for the different cutting force decompositions are assessed through the coefficients of determination. Due to signal noise the identification of the exact area of action in the measured signal is difficult. Therefore a signal range is defined where the norm of the cutting force is higher than 15 % of its maximum. Thus for the analyzed range the signals do not start at zero, see Figs. 8-10. Every time increment within this range is considered in the calculation of the coefficients of determination.

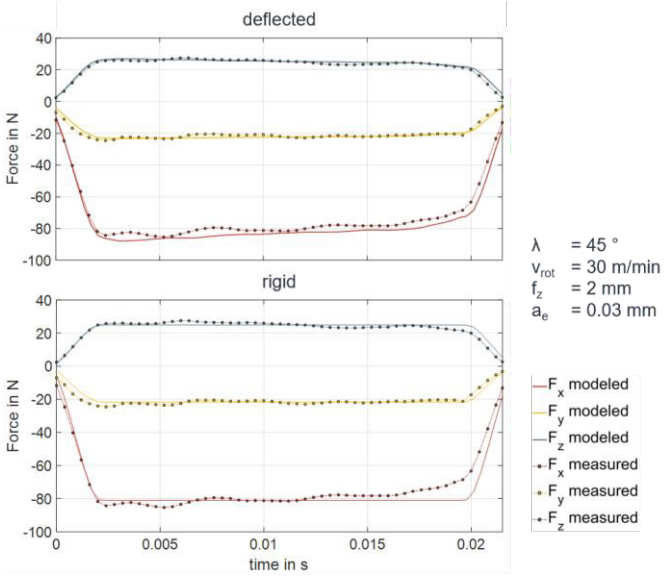

Fig. 8. Comparison of force prediction with and without deflection

First the coefficients of determination are calculated for all HFC tests of the experimental plan. In order to validate the transferability classic up-milling tests with the 45° tool and the 30° tool were analyzed. Fig. 9 shows the results of measurement and modeled prediction for the three cutting force components of DeCo-3.

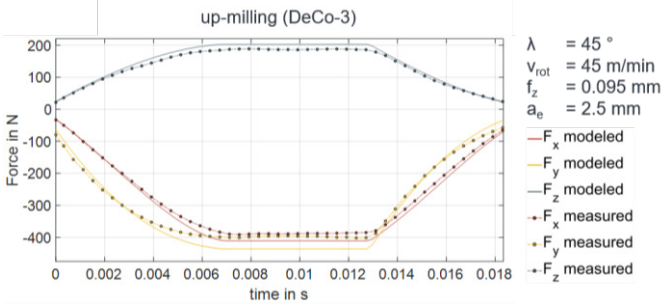

Fig. 9. Validation of cutting force prediction in up-milling process

Furthermore, another validation point was performed with the head of the ball end tool. The tool position was lifted to change the interacting cutting edge to the curved ball end part as well as the straight end mill part, see Fig. 10.

The best prediction is achieved by the force decomposition along the effective speed decomposition (DeCo-3). It allows adequate consideration of the changing sliding and normal speeds in their respective effective direction. The transferability from HFC to normal up-milling is successful in equally high quality for all three decompositions, see table 1. The transferability to another geometry, like for the ball nose tool, shows significant advantages of DeCo-3. The two decompositions DeCo-1 and DeCo-2 are not able to sufficiently predict the trend of force component F_z. In Fig. 10 significant deviations for this force component can be seen for DeCo-2. For DeCo-1 a similar tendency was identified. The results of the validation are listed in Table 1.

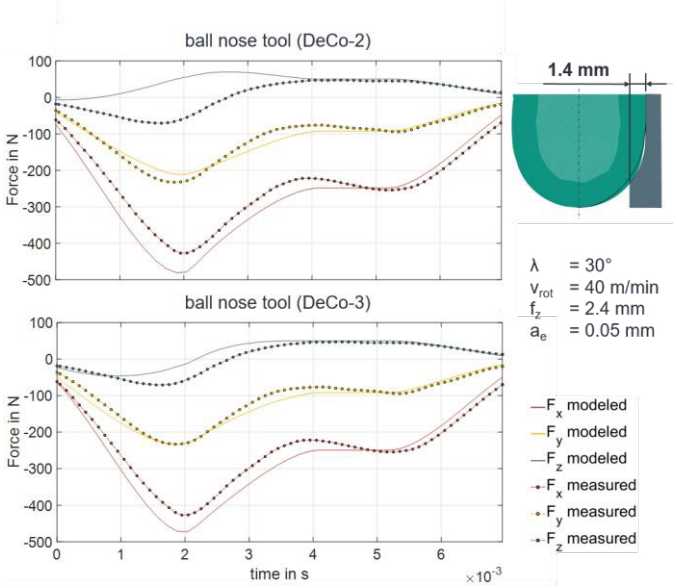

Fig. 10. Validation of cutting force prediction in ball end milling

Table 1. Coefficients of determination for the validation tests

Cutting force decomposition	Direction	R^2 - up-milling	R^2 - ball nose
(DeCo-1)	X	0.979	0.958
	Y	0.963	0.954
	Z	0.963	-
(DeCo-2)	X	0.979	0.899
	Y	0.964	0.924
	Z	0.959	-
(DeCo-3)	X	0.981	0.926
	Y	0.964	0.952
	Z	0.963	0.707

The consideration of tool and machine deflection shows a considerable influence on the local cutting parameters. With the consideration of deflection the decreasing force trend during tool interaction can be predicted, see Fig. 8. On the one hand, the areas of action change. On the other hand, the real chip thicknesses differ up to 18 % compared to the theoretical chip thicknesses, calculated with a rigid setup. Therefore it should be mentioned that the main influence on the chip thickness deviation is the cutting force difference between precut and measurement cut.

The forces of the measuring cut with radial infeed less than 0.05 mm are below the precut forces. Hence, if the deflection between tool and workpiece is higher in the precut than in the measurement cut, the real chip thickness in the test is not sufficiently estimated by a rigid model, see Fig. 7. Accordingly, experimental points with higher radial infeed than in the precut show the opposite behavior. This highlights the challenge to experimental setup and procedure to acquire reliable results especially for finish milling parameters.

The comparison of the fitted regression parameters, listed in Table 2, with and without considering deflection show a significant influence on the slope of the specific cutting forces. This is recognizable by the chip thickness exponents $m_{t,r,a}$ and suggests a rigid process modeling without consideration of deflection leads to cutting force models with inaccurate chip thickness consideration.

Table 2. Regression parameters for rigid and deflected modelling - DeCo-3

	K_t	m_t	m_{tne}	m_{tse}
rigid	**893**	**0.326**	0.343	- 0.448
deflected	**1246**	**0.162**	0.449	- 0.51
	K_r	m_r	m_{rne}	m_{rse}
rigid	**78**	**0.543**	1.069	- 1.054
deflected	**101**	**0.415**	1.143	- 1.092
	K_a	m_a	m_{ane}	m_{ase}
rigid	**379**	**0.409**	- 0.417	0.281
deflected	**507**	**0.258**	- 0.321	0.231

6. Conclusion

The new high feed peripheral milling experiment provides promising results for the analysis of the manufactured topography taking into account varying effective process parameters. With relatively few experimental points a statistically sound model can be fitted. The good suitability of the HFC experiments to analyze an adequate model for deflection and therefore the real chip thickness is a major advantage. Taking into account the deflection is important as a significant impact on the regression parameters and the decreasing force trend during tool interaction was shown.

The three compared force decompositions all show very good results when fitted with regression models to predict cutting forces for the same tool in a different process i.e. conventional up milling. However the proposed decomposition of the cutting forces according to the speed directions presents an advantage as it predicted cutting forces also for processes with a different tool geometry, like the head of a ball end mill, in good approximation. Of the three decompositions, only the speed decomposition based model allows to map the changing conditions due to differing sliding speeds on varying tool geometries. Therefore it was shown that this model can be transferred to other geometries and kinematics.

In further work the cutting force modeling will be expanded and analyzed in further detail in regard to the local effective mechanisms. Therefore the influence of the variation of effective rake and clearance angle, other helix angles, tool coatings and cutting edge preparations will be investigated. This will enable the transferability to other complex kinematics and geometries like those which are necessary for gear skiving, whirling and five axis simultaneous machining.

Acknowledgements

The authors wish to thank the German Research Foundation (DFG) for funding the project ”DFG-Transferprojekt-Taumelfräsen” (SCHU 101/69-1).

References

[1 Han, Zhenyu; Jin, Hongyu; Fu, Hongya (2015): Cutting force prediction models of metal machining processes: A review. In: 2015 International Conference on Estimation, Detection and Information Fusion (ICEDIF). 2015 International Conference on Estimation, Detection and Information Fusion (ICEDIF). Harbin, China, 10.01.2015 - 11.01.2015: IEEE, p. 323–328

[2] Merchant, M. Eugene (1945): Mechanics of the Metal Cutting Process. I. Orthogonal Cutting and a Type 2 Chip. In: *Journal of Applied Physics* 16 (5), p. 267–275.

[3]. Pratap, Tej; Patra, Karali (2017): Finite Element Method Based Modeling for Prediction of Cutting Forces in Micro-end Milling. In: *J. Inst. Eng. India Ser. C* 98 (1), p. 17–26.

[4]. Jin, Xiaoliang; Altintas, Yusuf (2012): Prediction of micro-milling forces with finite element method. In: *Journal of Materials Processing Technology* 212 (3), p. 542–552.

[5] Engin, S.; Altintas, Y. (2001): Mechanics and dynamics of general milling cutters. In: *International Journal of Machine Tools and Manufacture* 41 (15), p. 2195–2212.

[6] Campatelli, G.; Scippa, A. (2012): Prediction of Milling Cutting Force Coefficients for Aluminum 6082-T4. In: *Procedia CIRP* 1, p. 563–568.

[7] Altintas, Y.; Spence, A.; Tlusty, J. (1991): End Milling Force Algorithms for CAD Systems. In: *CIRP Annals* 40 (1), p. 31–34.

[8] Lazoglu, Ismail (2003): Sculpture surface machining: a generalized model of ball-end milling force system. In: *International Journal of Machine Tools and Manufacture* 43 (5), p. 453–462.

[9] Lee, P.; Altintaş, Y. (1996): Prediction of ball-end milling forces from orthogonal cutting data. In: *International Journal of Machine Tools and Manufacture* 36 (9), p. 1059–1072.

[10] Gradišek, Janez; Kalveram, Martin; Weinert, Klaus (2004): Mechanistic identification of specific force coefficients for a general end mill. In: *International Journal of Machine Tools and Manufacture* 44 (4), p. 401–414.

[11] Denkena, Berend; Vehmeyer, Jost; Niederwestberg, Daniel; Maaß, Peter (2014): Identification of the specific cutting force for geometrically defined cutting edges and varying cutting conditions. In: *International Journal of Machine Tools and Manufacture* 82-83, p. 42–49.

[12] Denkena, B.; Grove, T.; Pape, O. (2019): Optimization of complex cutting tools using a multi-dexel based material removal simulation. In: *Procedia CIRP* 82, p. 379–382.

[13] Vargas, Bruno; Zapf, Matthias; Klose, Jan; Zanger, Frederik; Schulze, Volker (2019): Numerical Modelling of Cutting Forces in Gear Skiving. In: *Procedia CIRP* 82, p. 455–460.

[14] Moges, Tesfaye M.; Desai, K. A.; Rao, P. V. M. (2018): Modeling of cutting force, tool deflection, and surface error in micro-milling operation. In: *Int J Adv Manuf Technol* 98 (9-12), p. 2865–2881.

[15] Kienzle, O.; Victor, H (1957): Spezifische Schnittkr¨afte bei der Metallbearbeitung. In:Werkstofftechnik und Maschinenbau 47 , Nr. H5, p.224–225.

[16] Moré, J.J., (1977): The Levenberg-Marquardt Algorithm: Implementation and Theory, *Numerical Analysis*, ed. G. A. Watson, Lecture Notes in Mathematics 630, Springer Verlag, p.105–116